

A simple approach to describe hadron production rates in inelastic pp and $p\bar{p}$ collisions

Yi-Jin Pei

I. Phys. Institut der RWTH, D-52074 Aachen, Germany

and

CERN, Ch-1211 Geneva 23, Switzerland

(e-mail: Yi-Jin.Pei@cern.ch)

Abstract

We show that the production rates of light-flavoured mesons and baryons in inelastic pp and $p\bar{p}$ collisions can be described by a simple approach used to describe data obtained in e^+e^- annihilation. Based on the idea of string fragmentation, the approach describes the production rates of light-flavoured mesons and baryons originating from fragmentation in terms of the spin, the binding energy of the particle, and a strangeness suppression factor. Apart from a normalization factor and the additional sea quark contribution in inelastic pp and $p\bar{p}$ collisions, pp , $p\bar{p}$ and e^+e^- data at various centre-of-mass energies are described simultaneously.

1 Introduction

The soft processes of the fragmentation of quarks and gluons into hadrons cannot be calculated with a perturbative approach and instead currently rely on phenomenological models. The most successful are the string [1] and the cluster [2] fragmentation models implemented in the Monte Carlo programs PYTHIA/JETSET [3] and HERWIG [4], respectively. However, these models require either a large number of free parameters in order to reproduce the measured hadron production rates (more dramatic in the case of PYTHIA/JETSET), or do not give a satisfactory description of baryon data in e^+e^- annihilation, as in the case of HERWIG (a review may be found in Ref. [5, 6]).

In Ref. [7] a simple approach based on the idea of string fragmentation to describe hadron production rates in e^+e^- annihilation is proposed. We consider that particle production proceeds in two stages, namely quark pair production in the colour string field and successive recombination. Quark pair production in the colour string field can be considered as a tunneling process. The probability of producing a $q\bar{q}$ pair is proportional to $\exp(-\pi m_q^2/\kappa)$, where m_q is the (constituent) quark mass, and κ the string constant. We assume that the probability of quarks recombining to a hadron with the mass M_h is proportional to $\exp(-E_{bind}/T)$, where T is the effective temperature in hadronization, and $E_{bind} = M_h - \sum_i m_{q_i}$ the hadron binding energy, which can be ascribed to the colour-magnetic hyperfine interaction ¹ [8].

The production rates of light-flavoured mesons and baryons from fragmentation can be described as

$$\langle N \rangle = C \cdot \frac{2J+1}{C_B} \cdot (\gamma_s)^{N_s} \cdot e^{-\frac{E_{bind}}{T}}, \quad (1)$$

where $\gamma_s = \exp[-\pi(m_s^2 - m_u^2)/\kappa]$ is the strangeness suppression factor, N_s the number of strange quarks contained in the hadron, and J the spin of the hadron. C is an overall normalization factor, which increases with the increasing centre-of-mass energy (reflecting the rise of multiplicities with increasing energy, which can be predicted by QCD [9]), and C_B is the relative normalization factor between mesons and baryons (for mesons $C_B = 1$). Our approach describes quite well the existing e^+e^- data on hadron production at various centre-of-mass energies. Furthermore, it can be applied to heavy flavour production and its predictions there also agree well with data.

Multiparticle production in hadron-hadron interactions with low-momentum transfer, which is still one of the least understood processes in high-energy physics, has been studied and compared with particle production in e^+e^- annihilation by many authors [10, 11, 12, 13, 14]. It is generally believed that the mechanism of hadronization is the same in all high-energy processes, and that all differences in particle composition can be traced to different initial parton configurations ². It is therefore important to test our approach with data obtained in hadron-hadron collisions.

In this paper, we first show some similarities between the hadron production rates measured in inelastic pp collisions and in e^+e^- annihilation. Then, taking into account the different initial

¹One could consider that the production probability of a hadron with a given quark content similar to the distribution of the number of atoms at different energy levels of the hyperfine splitting is determined by the Boltzmann distribution.

²The Lund string model [1, 3], for example, is one explicit realization of this concept.

parton configurations and the contribution from sea quarks, we apply our approach to data obtained in inelastic pp and p \bar{p} collisions.

2 Data on hadron production in pp and p \bar{p} collisions

The data on hadron production in inelastic pp and p \bar{p} collisions used in this analysis are listed in Tables 1–4. In some papers, listed in the Tables, pp data are given in terms of production cross sections instead of production rates. To calculate the production rate of hadrons per inelastic pp collision, we use the value of the total inelastic pp cross sections quoted in the papers, or the value from Ref. [15] at the corresponding centre-of-mass energy if inelastic pp cross sections are not given in the papers. When counting the hadron production rates, the decay products of K_S^0 , Λ , Σ^\pm , $\Xi^{0,-}$ and Ω^- (and their antiparticles) are not included in the papers. This is different from the counting procedure used for e^+e^- data.

The most complete set of data on hadron production in inelastic pp collisions consists of the LEBC-EHS results [16] at $p_{\text{LAB}} = 400$ GeV (centre-of-mass energy $\sqrt{s} = 27.4$ GeV), and the Fermilab 30-inch bubble chamber data [17] at $p_{\text{LAB}} = 405$ GeV ($\sqrt{s} = 27.6$ GeV). This data set can be compared with the LEP data [18], the most complete set of data on hadron production in e^+e^- annihilation. Although the type of interactions and the initial parton configuration in pp interactions with low-momentum transfer are different from those in e^+e^- annihilation, for a direct comparison we can however use hadrons which do not contain the valence quarks (u,d) in the proton, such as $\bar{u}s$, $\bar{d}s$ and $s\bar{s}$ mesons, and antibaryons. In most of the cases, such hadrons are either produced from fragmentation, or are decay products of other hadrons which are produced from fragmentation³. On the other hand, the contribution of the primary $q\bar{q}$ pair to the production rate of light-flavoured hadrons is small at LEP. It is therefore possible to use the following hadrons to compare directly hadron production from fragmentation in inelastic pp collisions and in e^+e^- annihilation:

Hadron	$n_{pp}(27.5\text{GeV})/n_{ee}(91\text{GeV})$	Hadron	$n_{pp}(27.5\text{GeV})/n_{ee}(91\text{GeV})$
K^-	0.19 ± 0.01	\bar{p}	0.13 ± 0.01
K^{*-}	0.25 ± 0.04	$\bar{\Lambda}$	0.11 ± 0.02
\bar{K}^{*0}	0.24 ± 0.04	$\bar{\Delta}^{--}$	0.20 ± 0.13
ϕ	0.18 ± 0.02	$\bar{\Sigma}^\pm$	0.35 ± 0.13

For all hadrons except the \bar{p} and $\bar{\Lambda}$, the ratio n_{pp}/n_{ee} is about the same within errors, indicating that hadron production from fragmentation in inelastic pp collisions and in e^+e^- annihilation differs only by a normalization factor, i.e., the available energy in fragmentation. For the \bar{p} and $\bar{\Lambda}$, this ratio is lower than that for other hadrons, mainly due to the different counting procedures used for decay products of the Λ , Σ^\pm , $\Xi^{0,-}$ and Ω^- (and their antiparticles) as mentioned above, and to the additional contribution to the \bar{p} and $\bar{\Lambda}$ from decays of c and b baryons in e^+e^- annihilation. If these two corrections are taken into account, the ratio n_{pp}/n_{ee} is then equal to 0.21 ± 0.02 for the \bar{p} ⁴. From the values of the ratio n_{pp}/n_{ee} listed above,

³The contribution of sea quarks and antiquarks to hadron production is small (see discussions in the next section)

⁴For the $\bar{\Lambda}$ the uncertainty of the corrections is large since the branching fractions $c(b)$ baryons $\rightarrow \bar{\Lambda}$ are not well known.

we see that the number of hadrons produced from fragmentation in inelastic pp collisions at $\sqrt{s} \simeq 27.5$ GeV is about 20% of that in e^+e^- annihilation at $\sqrt{s} = 91$ GeV. We will discuss this in more detail in the next section.

3 Analysis

We first consider hadron production in inelastic pp collisions. Similar to hadron production in e^+e^- annihilation, this process can also be considered to proceed in four steps: interaction between two initiator partons (valence quarks, gluons, sea quarks or antiquarks) with two beam remnants left behind, followed by a parton shower development from the initiator partons, and subsequently the transition from partons to hadrons. Finally, the unstable hadrons decay according to their branching ratios.

For a proton the possible scenarios for the initiator parton and beam remnant are the following:

1. If the initiator parton is a valence quark q_v , the beam remnant is simply a diquark composed of the two leftover valence quarks, i.e. either a ud or a uu diquark. The initiator parton and the diquark are at the two end-points of a string which is then hadronized in the usual way [3].
2. If the initiator parton is a sea quark q_s or antiquark \bar{q}_s , the beam remnant contains four quarks: $uud\bar{q}_s$ or $uudq_s$. Since the $q_s\bar{q}_s$ pair, to a first approximation, is in a colour-octet, the subdivision $uud+q_s$ (or $uud+\bar{q}_s$) is not allowed, since it would correspond to a colour-singlet $q_s\bar{q}_s$ [3]. Therefore uud will be subdivided into a quark (u or d) and a diquark (ud or uu). In this case in the beam remnant we have a diquark and two single quarks (or a quark and an antiquark), which will then be at the end-points of two strings⁵ and hadronized in the usual way. We introduce two free parameters for the fractions of the sea quarks: $f = f_u = f_d$ and $x_s = f_s/f$.
3. If the initiator parton is a gluon g , the beam remnant is a colour-octet uud state, which is subdivided into a quark and a diquark. The treatment is similar to that for scenario 1.

On average, the individual numbers of the primary quarks and diquarks in an inelastic pp collision are: $N_u = 2(\frac{2}{3} + f)$, $N_d = 2(\frac{1}{3} + f)$, $N_{\bar{u}} = N_{\bar{d}} = 2f$, $N_s = N_{\bar{s}} = 2x_s f$, $N_{uu} = 2 \times \frac{1}{3}$ and $N_{ud} = 2 \times \frac{2}{3}$.

Taking into account the numbers of the primary quarks and diquarks, hadron production in inelastic pp collisions can also be described by our approach discussed in Ref. [7]. For simplicity, as in Ref. [7], we apply our approach analytically to the data. Instead of using the parton distributions $p(x, Q^2)$ ($p = q_v, q_s, \bar{q}_s, g$), for the above three scenarios we use an averaged parameter C in Eq. (1), which is integrated over x . The total hadron rates are calculated as follows. Firstly we calculate the number of primary hadrons. Primary hadrons are defined as those which are not decay products of other hadrons, i.e. as hadrons originating

⁵Here we use the treatment of sea quarks and antiquarks as discussed in Ref. [19], which is different from the conventional way [3].

from fragmentation, or containing a primary quark or a diquark from the p in an inelastic pp collision. We use Eq. (1) to calculate the number of light-flavoured hadrons produced from fragmentation. Heavy quark production from fragmentation is strongly suppressed due to the term $\exp(-\pi m_q^2/\kappa)$ and can therefore be neglected. For hadrons which contain a primary quark q ($q = q_v, q_s, \bar{q}_s$) or a primary diquark $q_v^1 q_v^2$, we use Eq. (1) to determine their relative ratios, and then obtain their rates by normalizing the sum of the rates to the average number of q or $q_v^1 q_v^2$ in an inelastic pp collision. Compared to the production cross section of light-flavoured hadrons, the charm and bottom production cross sections in pp collisions are small [20] and can therefore be neglected in this analysis. The spin of the diquark is taken into account in the calculation. For example, the Λ contains a spin-0 ud and the Σ^0 a spin-1 ud diquark. All light-flavoured hadrons up to a mass of 2.5 GeV in the meson and baryon summary table of Ref. [15] are included in the calculation. Finally, we let all the primary hadrons decay according to their decay channels and branching ratios given in Ref. [15]. The decay chain stops when μ , π , K^\pm , K_L^0 , K_S^0 , Λ , Σ^\pm , $\Xi^{0,-}$, Ω^- (or their antiparticles) or stable particles are reached.

In the fit to pp data at $\sqrt{s} = 27.4\text{--}27.6$ GeV, we choose C , f and x_s as free parameters. For the other parameters in Eq. (1) we use the result of the fit to e^+e^- data [7]: $\gamma_s = 0.29 \pm 0.02$, $\Delta m = 0.161 \pm 0.024$ (GeV), $T = 0.298 \pm 0.015$ (GeV) and $C_B = 11.0 \pm 0.9$. In the fit these parameters are set to their central values since otherwise there would be too many free parameters which are highly correlated with each other, leading to unstable fit results. The value of m_s is set to 0.5 GeV⁶. The fit is performed by minimizing the error function

$$\chi^2 = \sum_i (N_i^{calc} - N_i^{meas})^2 / (\Delta N_i^{meas})^2, \quad (2)$$

where N_i^{calc} is the calculated rate, N_i^{meas} and ΔN_i^{meas} the measured rate and its error, respectively.

The fit results are listed in Table 5 and shown in Fig. 1. The value of the normalization factor C is equal to 0.042 ± 0.007 , where the error also includes the uncertainty on γ_s , Δm , T and C_B which are set to their central values in the fit. The ratio of this value and the value of C obtained from the fit to e^+e^- data at $\sqrt{s} = 91$ GeV [7] is $(19 \pm 3)\%$ (common systematic errors have been taken into account), which is in a good agreement with the value of n_{pp}/n_{ee} discussed in the previous section. From the fit, the probability that the initiator parton is a u (or d) sea quark is determined to be $f = 0.044 \pm 0.010$. The strange sea content is determined to be $x_s = f_s/f = 0.51 \pm 0.22$, which is consistent with the parametrization used in Ref. [21].

If we also choose the parameter T as a free parameter in the fit, we obtain $T = 0.271 \pm 0.010$ GeV, which is in agreement with the values of T obtained from the fits to e^+e^- data [7]. This indicates that the value of T is universal in different types of interactions.

As can be seen from Table 2 and Fig. 1, for most of the hadrons the calculated rate agrees well with the measurement (within two standard deviations). Only at three data points, namely π^+ , ρ^0 and Σ^{*-} , is the difference between the calculated and measured rates larger than three standard deviations. These three data points contribute more than half of the χ^2 value of the fit (49 out of the total χ^2 of 85 for 33 data points, fitted with three free parameters). Another major reason for the large χ^2 value is because the uncertainty of the calculated rates

⁶Since $\exp(-E_{bind}/T) = \exp(\sum_i m_u/T) \cdot \exp\{-[M_h - \sum_i (m_{q_i} - m_u)]/T\}$, the factor $\exp(\sum_i m_u/T)$ can be absorbed in C and C_B . The error function of the fit is mainly sensitive to the change in the mass difference $m_s - m_u$.

due to uncertainties on the mass, branching ratios and decay modes of the resonance states is not taken into account in the fit. If, for example, we introduce a 5% error on the number of secondary particles as the uncertainty of the calculated rates ($\Delta N_i^{calc} = 0.05 * (1 - f_i^{prim}) * N_i^{calc}$, where f_i^{prim} is the primary fraction of hadron i) and add it to the term ΔN_i^{meas} in Eq. (2), the χ^2/dof value of the fit is then reduced from 85/30 to 61/30, while the fit results remain essentially unchanged. Comparing the fit to almost the same data set with the same number of free parameters in Ref. [14], the χ^2/dof value of our fit is much lower ⁷ and our calculated rates are closer to the measured rates.

In the fit to pp and p \bar{p} data at the other centre-of-mass energies we choose only C as a free parameter because of the small number of data points available at some energies. The parameters f and x_s are set at the values obtained from the fit to pp data at $\sqrt{s} = 27.4$ – 27.6 GeV. In the pp data set at $\sqrt{s} = 52.5$ – 53.0 GeV, $f_2(1270)$, $K_2^{*\pm}(1430)$ and $\bar{K}_2^{*\pm}(1430)$ are not included in the fit as the results from Ref. [22] and [23] differ significantly. The treatment of initiator partons and beam remnants in p \bar{p} collisions is similar to that in pp collisions, with one of the two initiator partons and beam remnants replaced by their antiparticles. The fit results are listed in Tables 1, 3, 4 and 5. One can see that the calculated rates agree well with the measurements.

The fraction of primary hadrons is also given in Tables 1–4. Owing to different initial parton configurations, the fraction values in Tables 1–4 are different from the corresponding values for hadrons produced in e^+e^- annihilation at $\sqrt{s} = 91$ GeV (see the last column in Table 2):

- For mesons, and in inelastic pp collisions also antibaryons, the fraction value for pp (p \bar{p}) data is in general slightly higher than that for e^+e^- data, mainly due to the fact that the amount of c and b hadrons produced in pp (p \bar{p}) collisions is negligible. In contrast, in e^+e^- annihilation at $\sqrt{s} = 91$ GeV about 40% of the events contain c or b hadrons which decay to light-flavoured hadrons, leading to a lower value of the primary fraction of light-flavoured hadrons.
- For baryons which contain a uu ($\bar{u}\bar{u}$) or ud ($\bar{u}\bar{d}$) diquark, the fraction value for pp (p \bar{p}) data is much higher than that for e^+e^- data as a uu ($\bar{u}\bar{u}$) or ud ($\bar{u}\bar{d}$) diquark already exists in the initial configuration of inelastic pp (p \bar{p}) collisions. In contrast, for ddd ($\bar{d}\bar{d}\bar{d}$) or dds ($\bar{d}\bar{d}\bar{s}$) types of baryons, for example, the Σ^- , the fraction value can be lower than that for e^+e^- data as such baryons cannot be produced directly from the diquark in the p (\bar{p}), but can be decay products of the other baryons which are produced directly from the diquark in the p (\bar{p}).

4 Conclusions

We have shown that the production rates of light-flavoured mesons and baryons in inelastic pp and p \bar{p} collisions are described by a simple approach used to describe e^+e^- data. Taking into account the different initial parton configurations and the additional sea quark contribution in

⁷Note in Ref. [14] a ΔN_i^{calc} term has been taken into account in the fit. In some cases, for example, for ρ^0 and Δ^{++} , ΔN_i^{calc} is much larger than ΔN_i^{meas} .

inelastic pp and $p\bar{p}$ collisions, pp , $p\bar{p}$ and e^+e^- data on the production of light-flavoured hadrons at various centre-of-mass energies are described simultaneously (apart from a normalization factor, which reflects the rise of multiplicities with increasing energy). Moreover, as shown in Ref. [7], data on heavy flavour production in e^+e^- annihilation are also described by our approach. All this shows that our approach can provide a universal description of hadron production, irrespective of the type of the interaction and the initial parton configuration in various interactions.

Acknowledgements

We are grateful to F. Becattini, T. Hebbeker, R.J. Hemingway and T. Sjöstrand for useful discussions. We also wish to thank J. Navarria for a careful reading of the draft of this paper.

References

- [1] B. Andersson et al., Phys. Rep. **97** (1983) 31.
- [2] G. Marchesini and B.R. Webber, Nucl. Phys. **B238** (1984) 1.
- [3] T. Sjöstrand, Comput. Phys. Commun. **82** (1994) 74;
T. Sjöstrand, *PYTHIA 5.7 and JETSET 7.4*, CERN-TH/93-7112.
- [4] G. Marchesini et al., Comput. Phys. Commun. **67** (1992) 465.
- [5] T. Sjöstrand, Preprint LU TP 95-19.
- [6] Y.J. Pei, *Particle Composition and Spectra at LEP1*, L3 Internal Note 1912⁸, a slightly modified version can be found in CERN Report CERN 96-01, Vol. 2, 109.
- [7] Y.J. Pei, Z. Phys. **C72** (1996) 39.
- [8] G. Gasiorowicz and J.L. Rosner, Am. J. Phys. **49** (1981) 954.
- [9] B.R. Webber, Phys. Lett. **B143** (1984) 501 and references therein.
- [10] M. Basile et al., Phys. Lett. **B95** (1980) 311 and Lett. Nuovo Cimento **41** (1984) 293.
- [11] M. Bardadin-Otwinowska, M. Szczekowski and A.K. Wroblewski, Z. Phys. **C13** (1982) 83.
- [12] P.V. Chliapnikov and V.A. Uvarov, Phys. Lett. **B251** (1990) 192.
- [13] M. Szczekowski, Phys. Lett. **B359** (1995) 387.
- [14] F. Becattini and U. Heinz, hep-ph/9702274 and Firenze preprint DFF 268/02/1997, submitted to Z. Phys. C.
- [15] Particle Data Group, *Review of Particle Properties*, Phys. Rev. **D54** (1996).
- [16] LEBC-EHS Collaboration, M. Aguilar-Benitez et al., Z. Phys. **C50** (1991) 405 and references therein.
- [17] H. Kichimi et al., Phys. Rev. **D20** (1979) 37.
- [18] A. De Angelis, CERN-PPE/95-135.
- [19] G. Ingelman, A. Edin and J. Rathsman, DESY Preprint 96-057.
- [20] LEBC-MPS Collaboration, R. Ammar et al., Phys. Rev. Lett. **61** (1988) 2185.
- [21] A.D. Martin and W.J. Stirling, Phys. Rev. **D51** (1995) 4756.
- [22] D. Drijard et al., Z. Phys. **C9** (1981) 293.
- [23] A. Böhm et al., Phys. Rev. Lett. **41** (1978) 1761.
- [24] S. Barish et al., Phys. Rev. **D9** (1974) 2689.

⁸On WWW: <http://l3www.cern.ch/homepages/peiyj/ps/lep1.ps>.

- [25] NA5 Collaboration, J. Allday et al., *Z. Phys.* **C40** (1988) 29.
- [26] K. Jaeger et al., *Phys. Rev.* **D11** (1975) 2405.
- [27] R. Singer et al., *Phys. Lett.* **B60** (1975) 385.
- [28] U. Amaldi and K.R. Schubert, *Nucl. Phys.* **B166** (1980) 301.
- [29] A.M. Rossi et al., *Nucl. Phys.* **B84** (1975) 269.
- [30] T. Kafka et al., *Phys. Rev.* **D19** (1979) 76.
- [31] F. Lo Pinto et al., *Phys. Rev.* **D22** (1980) 573.
- [32] EHS-RCBC Collaboration, J.L. Bailly et al., *Z. Phys.* **C23** (1984) 205.
- [33] EHS-RCBC Collaboration, M. Asai et al., *Z. Phys.* **C27** (1985) 11.
- [34] UA5 Collaboration, R.E. Ansorge et al., *Nucl. Phys.* **B328** (1989) 36 and references therein.

Hadron	Rate Measured	Rate Calculated	Primary Fraction Calculated	References
$\sqrt{s} = 19.4\text{--}19.7$ GeV ($\sigma_{inel} = 32.1$ mb [24])				
Charged	7.68 ± 0.06	7.53		[24, 25]
Neg. charged	2.85 ± 0.03	2.90		[24, 25]
γ	6.68 ± 0.48	6.75		[26]
K_S^0	0.174 ± 0.011	0.205	0.28/0.30 ^(a)	[25, 26]
ρ^0	0.33 ± 0.06	0.39	0.49	[27]
Λ	0.098 ± 0.010	0.124	0.27	[25, 26]
$\bar{\Lambda}$	0.014 ± 0.004	0.011	0.15	[25, 26]
$\sqrt{s} = 23.3\text{--}23.7$ GeV ($\sigma_{inel} = 32.21$ mb [28])				
Charged	9.24 ± 1.39	8.61		[29]
π^0	3.42 ± 0.62	3.79	0.17	[30]
π^+	3.71 ± 0.37	3.67	0.19	[29]
π^-	3.27 ± 0.33	3.14	0.17	[29]
K_S^0	0.214 ± 0.025	0.250	0.28/0.30 ^(a)	[31]
K^+	0.337 ± 0.051	0.344	0.33	[29]
K^-	0.209 ± 0.031	0.212	0.28	[29]
$K^{*\pm}$	0.137 ± 0.043	0.215	0.60/0.67 ^(b)	[31]
p	1.63 ± 0.24	1.10	0.24	[29]
\bar{p}	0.085 ± 0.013	0.063	0.16	[29]
Λ	0.112 ± 0.016	0.131	0.27	[31]
$\bar{\Lambda}$	0.020 ± 0.004	0.018	0.15	[31]
$\Sigma^{*\pm}$	0.017 ± 0.012	0.021	1.00	[31]
$\bar{\Sigma}^{*\pm}$	0.014 ± 0.011	0.004	1.00	[31]
$\sqrt{s} = 26.0$ GeV ($\sigma_{inel} = 32.8$ mb [32])				
Charged	9.06 ± 0.09	8.92		[32]
Neg. charged	3.53 ± 0.05	3.60		[32]
K_S^0	0.26 ± 0.01	0.26	0.28/0.30 ^(a)	[33]
Λ	0.12 ± 0.02	0.13	0.26	[33]
$\bar{\Lambda}$	0.013 ± 0.004	0.020	0.15	[33]
(a) Primary fraction of K^0 and \bar{K}^0 , respectively.				
(b) Primary fraction of K^{*-} and K^{*+} , respectively.				

Table 1: Average hadron production rates per inelastic pp collision at various centre-of-mass energies (excluding charge conjugates and antiparticles if not indicated), compared with the calculated values. The fraction of primary hadrons obtained from the fit is also shown. For the calculated rates and fractions see discussions in Section 3.

Hadron	Rate Measured	Rate Calculated	Prim. Fraction Calculated	References	Prim. Fraction e ⁺ e ⁻ [7]
$\sqrt{s} = 27.4\text{--}27.6$ GeV ($\sigma_{inel} = 32.8$ mb [16])					
π^0	3.87 ± 0.12	3.82	0.17	[16]	0.16
π^+	4.10 ± 0.11	3.70	0.19	[16]	0.18
π^-	3.34 ± 0.08	3.17	0.17	[16]	0.18
K_S^0	0.232 ± 0.011	0.252	0.28/0.30 ^(a)	[17]	0.25
K^+	0.331 ± 0.016	0.346	0.33	[16]	0.23
K^-	0.224 ± 0.011	0.215	0.28	[16]	0.23
η	0.30 ± 0.02	0.33	0.28	[16]	0.30
ρ^0	0.385 ± 0.018	0.460	0.50	[16]	0.47
ρ^+	0.552 ± 0.082	0.490	0.54	[16]	0.58
ρ^-	0.354 ± 0.058	0.408	0.48	[16]	0.58
K^{*0}	0.120 ± 0.021	0.117	0.59	[16]	0.49
\bar{K}^{*0}	0.090 ± 0.016	0.079	0.59	[16]	0.49
K^{*+}	0.132 ± 0.016	0.137	0.67	[16]	0.50
K^{*-}	0.088 ± 0.012	0.080	0.60	[16]	0.50
ω	0.391 ± 0.024	0.421	0.52	[16]	0.48
ϕ	0.0189 ± 0.0018	0.0175	1.00	[16]	0.64
$f_0(980)$	0.023 ± 0.008	0.035	1.00	[16]	0.99
$f_2(1270)$	0.092 ± 0.012	0.090	0.77	[16]	0.78
$K_2^{*\pm}(1430)$	0.11 ± 0.05	0.04	1.00	[17]	1.00
p	1.20 ± 0.097	1.11	0.24	[16]	0.12
\bar{p}	0.063 ± 0.002	0.064	0.16	[16]	0.12
Λ	0.125 ± 0.008	0.131	0.27	[17]	0.12
$\bar{\Lambda}$	0.020 ± 0.004	0.018	0.15	[17]	0.12
Σ^+	0.048 ± 0.015	0.039	0.48	[16]	0.42
Σ^-	0.013 ± 0.006	0.021	0.10	[16]	0.42
Δ^{++}	0.218 ± 0.0031	0.214	0.83	[16]	0.69
$\bar{\Delta}^{--}$	0.0128 ± 0.0049	0.0105	0.72	[16]	0.69
Δ^0	0.141 ± 0.008	0.134	0.73	[16]	0.69
$\bar{\Delta}^0$	0.0336 ± 0.010	0.011	0.71	[16]	0.69
Σ^{*+}	0.0204 ± 0.0024	0.0193	1.00	[16]	0.91
Σ^{*-}	0.0100 ± 0.0018	0.0022	1.00	[16]	0.91
$\bar{\Sigma}^{*\pm}$	0.0078 ± 0.0025	0.0045	1.00	[16]	0.91
$\Lambda(1520)$	0.0171 ± 0.0031	0.0161	0.83	[16]	0.71

(a) Primary fraction of K^0 and \bar{K}^0 , respectively.

Table 2: Average hadron production rates per inelastic pp collision at $\sqrt{s} = 27.4\text{--}27.6$ GeV (excluding charge conjugates and antiparticles if not indicated), compared with the calculated values. The fraction of primary hadrons obtained from the fit is also shown. For the calculated rates and fractions see discussions in Section 3. For comparison, the fraction of primary hadrons obtained from the fit to e⁺e⁻ data at 91 GeV [7] is also given in the last column (the fraction values have been averaged for baryons belonging to the same isospin multiplet).

Hadron	Rate Measured	Rate Calculated	Primary Fraction Calculated	References
$\sqrt{s} = 30.6$ GeV				
Charged	10.07 ± 1.51	9.87		[29]
π^+	4.07 ± 0.41	4.21	0.20	[29]
π^-	3.65 ± 0.37	3.68	0.18	[29]
K^+	0.367 ± 0.055	0.400	0.33	[29]
K^-	0.244 ± 0.037	0.269	0.29	[29]
p	1.63 ± 0.24	1.13	0.24	[29]
\bar{p}	0.108 ± 0.016	0.091	0.16	[29]
$\sqrt{s} = 44.6$ GeV				
Charged	10.99 ± 1.65	10.82		[29]
π^+	4.45 ± 0.45	4.62	0.20	[29]
π^-	4.09 ± 0.41	4.09	0.18	[29]
K^+	0.411 ± 0.062	0.443	0.33	[29]
K^-	0.286 ± 0.043	0.312	0.29	[29]
p	1.62 ± 0.24	1.15	0.24	[29]
\bar{p}	0.132 ± 0.020	0.112	0.16	[29]
$\sqrt{s} = 52.5\text{--}53.0$ GeV ($\sigma_{inel} = 35.0$ mb [15])				
Charged	11.47 ± 1.72	11.24		[29]
π^+	4.68 ± 0.47	4.80	0.20	[29]
π^-	4.29 ± 0.43	4.27	0.18	[29]
K_S^0	0.329 ± 0.071	0.359	0.29/0.31 ^(a)	[22]
K^+	0.430 ± 0.065	0.462	0.33	[29]
K^-	0.306 ± 0.046	0.330	0.29	[29]
ρ^0	0.63 ± 0.14	0.62	0.51	[22]
\bar{K}^{*0}	0.123 ± 0.028	0.123	0.60	[22]
ϕ	0.037 ± 0.010	0.026	1.00	[22]
$f_2(1270)^{(b)}$	0.154 ± 0.034	0.122	0.77	[22]
$f_2(1270)^{(b)}$	0.075 ± 0.007	0.122	0.77	[23]
$K_2^{*\pm}(1430)^{(b)}$	0.0044 ± 0.0017	0.0264	1.00	[23]
$\bar{K}_2^{*\pm}(1430)^{(b)}$	0.028 ± 0.007	0.0205	1.00	[22]
$\bar{K}_2^{*\pm}(1430)^{(b)}$	0.0031 ± 0.0015	0.0205	1.00	[23]
p	1.62 ± 0.24	1.16	0.24	[29]
\bar{p}	0.144 ± 0.022	0.121	0.16	[29]
(a) Primary fraction of K^0 and \bar{K}^0 , respectively.				
(b) Not included in the fit.				

Table 3: Average hadron production rates per inelastic pp collision at various centre-of-mass energies (excluding charge conjugates and antiparticles if not indicated), compared with the calculated values. The fraction of primary hadrons obtained from the fit is also shown. For the calculated rates and fractions see discussions in Section 3.

Hadron	Rate Measured	Rate Calculated	Primary Fraction Calculated	References
$\sqrt{s} = 200$ GeV				
Charged	21.4 ± 0.4	21.4		[34] ^(a)
K_S^0	0.75 ± 0.09	0.78	0.31	[34]
n	0.75 ± 0.10	0.73	0.19	[34] ^(b)
Λ	0.23 ± 0.06	0.16	0.20	[34]
Ξ^-	0.015 ± 0.015	0.007	0.50	[34]
$\sqrt{s} = 546$ GeV				
Charged	29.4 ± 0.3	29.4		[34] ^(a)
K_S^0	1.12 ± 0.08	1.12	0.31	[34]
Λ	0.265 ± 0.055	0.205	0.19	[34]
Ξ^-	0.05 ± 0.015	0.011	0.50	[34]
$\sqrt{s} = 900$ GeV				
Charged	35.6 ± 0.9	35.7		[34] ^(a)
K_S^0	1.37 ± 0.13	1.38	0.31	[34]
n	1.0 ± 0.2	1.1	0.18	[34] ^(b)
Λ	0.38 ± 0.08	0.24	0.18	[34]
Ξ^-	0.035 ± 0.020	0.014	0.50	[34]
(a) The average charged multiplicity value quoted in this reference is increased by one to include the leading particles.				
(b) The average production rate of the neutron quoted in this reference is increased by 0.5 to include the leading particles.				

Table 4: Average hadron production rates per non-single-diffractive $p\bar{p}$ event at various centre-of-mass energies (excluding charge conjugates and antiparticles), compared with the calculated values. The fraction of primary hadrons obtained from the fit is also shown. For the calculated rates and fractions see discussions in Section 3.

$\sqrt{s}(\text{GeV})$	C	f	x_s	χ^2/dof
pp				
19.4–19.7	0.026 ± 0.004	0.044 (fixed)	0.51 (fixed)	25/6
23.3–23.7	0.041 ± 0.006	0.044 (fixed)	0.51 (fixed)	16/13
26.0	0.046 ± 0.007	0.044 (fixed)	0.51 (fixed)	7/4
27.4–27.6	0.042 ± 0.007	0.044 ± 0.010	0.51 ± 0.22	85/30
30.6	0.060 ± 0.010	0.044 (fixed)	0.51 (fixed)	6/6
44.6	0.074 ± 0.014	0.044 (fixed)	0.51 (fixed)	6/6
52.5–53.0	0.080 ± 0.010	0.044 (fixed)	0.51 (fixed)	7/10
p \bar{p}				
200	0.229 ± 0.035	0.044 (fixed)	0.51 (fixed)	2/4
546	0.347 ± 0.053	0.044 (fixed)	0.51 (fixed)	8/3
900	0.439 ± 0.066	0.044 (fixed)	0.51 (fixed)	4/4

Table 5: Results of the fit to pp and p \bar{p} data obtained at various centre-of-mass energies. The errors given in the Table also include the uncertainty on the parameters which are set to their central value in the fit.

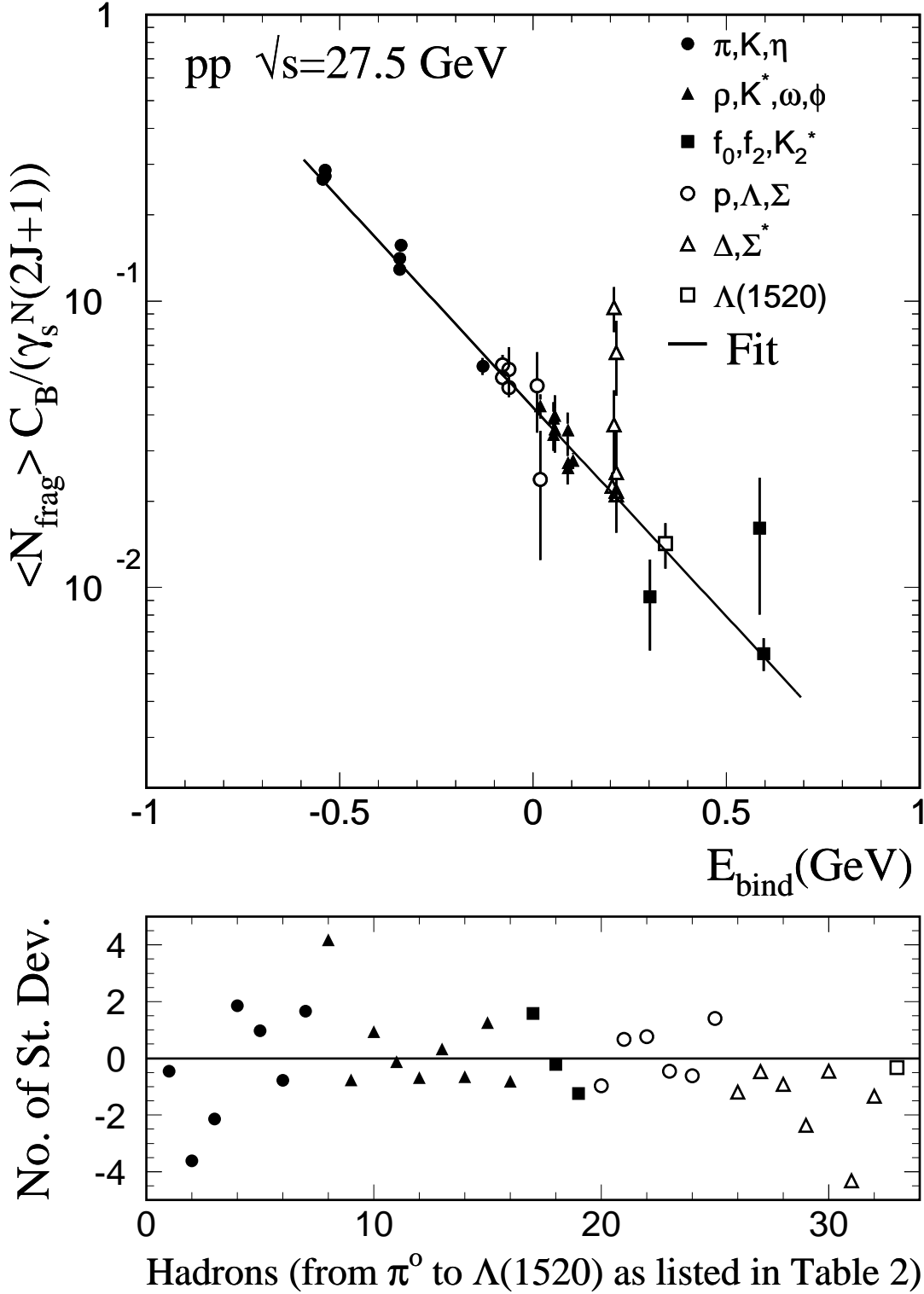


Figure 1: The upper plot shows the average hadron production rates of light-flavoured hadrons originating from fragmentation at $\sqrt{s} = 27.4\text{--}27.6$ GeV in inelastic pp collisions (measured value \times fraction of hadrons originating from fragmentation as determined by the fit), multiplied by the factor $C_B / [\gamma_s^{N_s} (2J + 1)]$ (see Eq. (1)), as a function of the binding energy of hadrons. The fit results are shown as the line. The lower plot shows the difference between the predicted and measured rates in terms of the number of standard deviations.